Lifetime Maximization in Rechargeable Wireless Sensor Networks with Charging Interference

Yi QU*, Ke XU*, Haiyang WANG†, Dan WANG‡, Bo WU*
*Department of Computer Science & Technology, Tsinghua University, P. R. China
†Department of Computer Science, University of Minnesota at Duluth, USA
‡Department of Computing, Hong Kong Polytechnic University, P. R. China
Email:{quy11,wub14}@mails.tsinghua.edu.cn, xuke@mail.tsinghua.edu.cn,
haiyang@d.umn.edu, csdwang@comp.polyu.edu.hk

***Abstract*—Radio Frequency based Wireless Power Transfer (RF-WPT) technology is recognized as a promising way to charge low-power wireless devices. But the application of RF-WPT in wireless sensor networks also introduces charging interference to wireless communications. The network lifetime maximization by jointly considering wireless charging and data transmission under interference concerns, however, has seldom been examined. In this paper, we take initial steps to consider communication and charger scheduling together in wireless sensor networks. We propose a smart interference-aware scheduling to maximize the network lifetime and avoid potential data loss caused by charging interference. The evaluation result indicates that the proposed design can guarantee 99% optimality and significantly improve network lifetime.**

I. Introduction

The development of Radio Frequency based Wireless Power Transfer(RF-WPT) provides a convenient means to charge low-power electronics in next generation wireless networks [13] [21]. Different from traditional magnetic resonant coupling approaches [10], RF-WPT is a lightweight technique that is suitable for low-power RFIDs and sensors [9] [13] [21]. However, it introduces higher degree of interference to wireless communications. In particular, the study from Naderi *et al.* [15] showed that RF energy transfer would cause data loss and largely reduce the wireless throughput. A smart scheduling between RF charging and data transmission is therefore required to bring RF-WPT deployments into reality.

In this paper, we take initial steps to investigate the potential benefit from jointly considering data communication and charger scheduling together under interference concerns. Based on our model analysis, we find that the lifetime maximization problem can hardly be solved in polynomial time due to the time-dependent constraints. To address this issue, we carefully transform the time-dependent continuous problem into a time-independent discrete problem. We show that the maximum system lifetime (in the original problem) can be easily obtained by solving the time-independent discrete problem. To further reduce the complexity of the problem, we relax the energy constraint of the original problem and simplify the charger's traveling path to a single TSP(*Traveling Salesman Problem*) path. We then construct a linear programming problem and prove that its optimal solution is equal to the relaxed problem. Based on this analysis, we finally propose a near optimal solution to the original problem with theoretically provable optimality $1 - \frac{\phi}{W}$, where W is an arbitrary positive integer and ϕ is determined by system properties such as the maximum charging duration. The contributions of this paper are summarized as follows:

- To the best of our knowledge, this is the first work that maximizes network lifetime in RF-WPT deployment under practical charging interference concerns.
- Our step-by-step model analysis shows that the complex joint optimization can be reasonably approximated into a simple linear programming problem.
- We develop a near optimal solution to the lifetime maximization problem with 99% optimality in RF-WPT deployment.

The rest of this paper is organized as follows: In section 2, we present related works. Section 3 discusses the system model. After that, the lifetime maximization problem is formulated in section 4. Section 5 explores a near optimal solution with guaranteed performance bound. This solution is then evaluated in section 6. Section 7 further discusses some practical issues in the system deployment and section 8 concludes the paper.

II. Related Work

A. RF-WPT

Since Maxwell formulated his famous equations in 1862, which formed the theoretical basis of RF-WPT, there has been a large body of works focus on this topic. In 1960s, Brown first developed a rectenna to receive and rectify power carried by high-frequency microwaves [2]. Although 40%-80% power transmission efficiency was observed, Brown's experiments caused unacceptable cost since large-scale peripheral devices were included. In the modern society, probably the most well-known commercial application of RF-WPT is RFID, where the RFID tags collect energy from interrogating radio waves and communicate exclusively with the RFID reader. By harvesting energy from ambient RF signals, Liu *et al.* [13] extended the traditional RFID tag with incomplete functions to a mini-computer with full computation, communication and control abilities.

Compared to magnetic resonant coupling approaches proposed by Kurs *et al.* [10], RF-WPT is recognized as the most suitable way to charge devices with ultra-low power requirements such as sensors and RFIDs [9] [13] [21]. This is due to the simplicity of RF-WPT that neither large coils (with

diameter of 0.6m in [10]) nor scrupulous resonance alignment is needed. Most importantly, RF-WPT brings about minimal cost increase, because it can be implemented by adding several basic electronic elements such as rectifier, capacitors and diodes to the existing circuits [9].

B. Charging Interference

In practice, there is no exclusive spectrum allocated for power transfer, and most RF-WPT systems operate at ISM(*Industry, Science and Medical*) band, which is already crowded with communication systems. Another factor that deteriorates the situation is that RF signals emitted for power transfer always exhibit higher signal strength than low-power data communications. Without special care, data transmissions will be heavily interfered after a mobile charger is introduced. For example, through experimental studies, Naderi *et al.* [14] showed that RF energy transfer would cause data loss and largely reduce the wireless throughput. The study in [15] reported similar phenomena.

Although charging interference can be partially alleviated by allocating non-intersect spectrums for power transfer and data communication, it causes severe spectrum efficiency problems. Based on results in [14], as to a rechargeable sensor network operating at 915 MHz, to ensure high quality communication, only 54% channel can be used for throughput if we allocate 912-918 MHz for RF-WPT. Note that 6 MHz band is also very limited for power transfer. In this paper, we avoid this kind of interference alleviation methods.

C. Adoption in WSNs

Recently, a flourish of research efforts have been paid to apply WPT in WSNs [19] [22] [6] [7] [5] [4]. In [19], a mobile wireless charging vehicle (WCV) is introduced and sensor batteries are replenished in a periodical manner. Adopted in small-scale networks, WCV ensured sensors stay operational forever. Mathematical study in [22] proved that bundling the base station on the WCV could further promote network performances. Aiming at the maximum network utility, an anchor-point based mobile data gathering scheme is proposed in [6], which achieves finer scalability and can be adopted in larger networks. Different from mobile charger approaches, He *et al.* [7] considered the charger deployment problem in static scenarios, which also ensured enough power transfer for sensor networks. Moreover, Fu *et al.* [5] studied the minimum charging delay problem while Dai *et al.* [4] attempted to transfer maximum power under a predefined electromagnetic radiation threshold.

In conclusion, existing studies mainly concentrate on sensor-charger cooperation, how to avoid charging interference has seldom been examined. This paper makes up the research gap in this area.

III. Mathematical Model

Considering the complexity of the system model, we introduce it in the following orders. In section III-A, we first describe the basic network model without energy charging. After a mobile charger is introduced, the charger mobility is presented in section III-B. Then, in section III-C, we focus on charging interference. In section III-D, we describe data communications under charging interference concerns. Lastly, sensor's energy profiles are illustrated in Section III-E.

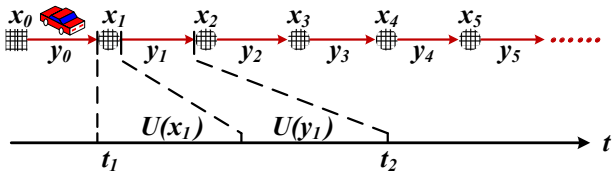

Fig. 1. The charger's traveling path consists of sojourn point x_l and path segment y_l. Diamond and circles represent the location of the sink (x_0) and sensors ($x_1, x_2, ...$). The car represents the mobile charger.

A. Basic Network Model

We consider a set of wireless sensors N initially equipped with rechargeable batteries and randomly deployed over a two-dimensional area. Each sensor $i \in N$ generates monitoring data with a rate of g_i, and all sensory data are forwarded to the sink. Denote $g_{ij}(t)$ the data rate from sensor i to j at time t ($i, j \in N, i \neq j$). Specifically, $g_{i0}(t)$ represents the data rate from sensor i to the sink. Then, the flow conservation equation at sensor i can be presented as [18]:

$$\sum_{k \in N}^{k \neq i} g_{ki}(t) + g_i = \sum_{j \in N}^{j \neq i} g_{ij}(t) + g_{i0}(t) \tag{1}$$

Denote $e_i(t)$ the energy consumption rate for sensor i at time t, in this paper, we adopt the following energy consumption model [19]:

$$e_i(t) = \sum_{k \in N}^{k \neq i} \rho g_{ki}(t) + \sum_{j \in N}^{j \neq i} C_{ij} g_{ij}(t) + C_{i0} g_{i0}(t) \tag{2}$$

where ρ is the energy consumption rate for receiving a unit of data rate and C_{ij} is the energy consumption rate for transmitting a unit of data rate from sensor i to sensor j. Specifically, $C_{ij} = \beta_1 + \beta_2 d_{ij}^{\alpha}$, where d_{ij} is the distance between sensor i and j, β_1 and β_2 are coefficients, and α is the path loss index.

B. Charger Mobility

Let the charger start from the sink, travel within the network area, visit sensors and terminate at the end of the network lifetime. When the charger visits a sensor i, it sojourns to charge i's battery. Then, it leaves sensor i and moves to the next sensor. The charger's traveling path consists of x_l and y_l ($l \in L$), where L is the sensor sequence that the charger will visit, x_l is a sojourn point and y_l is the path segment between x_l and x_{l+1} (see Fig. 1). Suppose the charger arrives at x_l at $t = t_l$ and the sojourn duration is $U(x_l)$, then we have $t_{l+1} - t_l = U(x_l) + U(y_l)$, where $U(y_l)$ is the time spent to traverse y_l.

Practically, charging rates decrease exponentially with increasing charging distances [7] [15]. For the sake of effective charging, similar to [6] [19], we assume that a sensor can be charged only when the charger visits it. Thus, the energy transfer model in [7] can be simplified as $K_{il} = \varpi U(x_l)$, where ϖ is the energy transfer rate, K_{il} is the energy charged

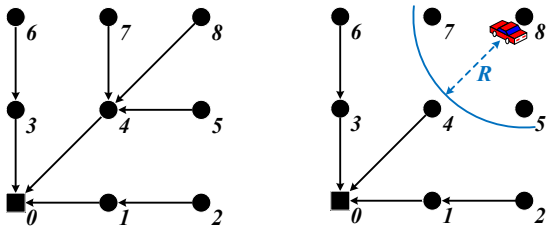

(a) Network topology. (b) Charging interference.

Fig. 2. In this example, the network topology is given in (a) and a mobile charger sojourns at x_8 to visit sensor 8 in (b). Around the charger, sensor 5, 7, 8 are interfered. Solid diamond and circles represent sink and sensors, respectively.

for sensor i when the charger sojourns at x_l. In particular, $K_{il} > 0$ implies that the charger sojourns at x_l to visit sensor i. Otherwise, $K_{il} = 0$.

C. Charging Interference

Whenever the charger transfers energy for a sensor, data communications around it will be interfered. Denote the interference radius as R and the distance between x_l and sensor i as d_{il}. When the charger sojourns at x_l, only if $d_{il} \geq R$, sensor i's data can be transmitted (or received) without loss. Let N_l be the interfered sensor set, then we have $N_l = \{i | i \in N, d_{il} < R\}$. Take Fig. 2 as an example, the charger is visiting sensor 8 and $N_8 = \{5, 7, 8\}$.

Analyzing charger mobility shown in Fig. 1, we find that each charging duration $U(x_l)$ is followed by a traveling duration $U(y_l)$. During $U(y_l)$, neither power transfer nor interference exists. We can leveraging this regularity to avoid data loss caused by charging interference. Specifically, when data communications are interfered, sensors temporarily store all to-be-transmitted data. Whenever the interference disappears, the stored data can be released from local storage and transmitted toward the sink. As shown in Fig. 2(b), sensor 5, 7 and 8 store data when the charger is charging sensor 8. When the charger finishes charging and moves to the next sensor, all stored data in sensor 5, 7 and 8 can be forwarded to the sink.

D. Data Communication

For a given x_l, the data routing model during $[t_l, t_l + U(x_l)]$ can be extended from the basic model as follows. For sensor i, we have:

$$\sum_{k \in N}^{k \neq i} g_{ki}(t) + g_i = \sum_{j \in N}^{j \neq i} g_{ij}(t) + g_{i0}(t) + g_i^s(t) \qquad (3)$$

where $g_i^s(t)$ is the data storing rate. For sensor $i \notin N_l$, there is no necessary to store data, thus $g_i^s(t) = 0$. As to interfered sensor $i \in N_l$, data transmission and reception are prohibited to avoid possible loss. Namely, $\sum_{k \in N}^{k \neq i} g_{ki}(t) = 0$, $\sum_{j \in N}^{j \neq i} g_{ij}(t) = 0$ and $g_{i0}(t) = 0$. Thus we have $g_i^s(t) = g_i$.

During $[t_l, t_l + U(x_l)]$, interfered sensor $i \in N_l$ stores sensory data to its storage. And longer sojourn duration $U(x_l)$ will lead to larger storage occupation. Since a sensor's storage is also scarce, a maximum sojourn time U_{max} is set to avoid excessive storage occupation:

$$U(x_l) \leq U_{max}, \quad \forall l \in L \qquad (4)$$

When the charger finishes charging at x_l and moves to the next sensor during $[t_l + U(x_l), t_{l+1}]$, none sensor will be interfered. During this interval, for sensor i, we have the following flow conservation equation:

$$\sum_{k \in N}^{k \neq i} g_{ki}(t) + g_i = \sum_{j \in N}^{j \neq i} g_{ij}(t) + g_{i0}(t) - g_i^r(t) \qquad (5)$$

where $g_i^r(t)$ is the data releasing rate. To avoid unacceptable delay, data stored during $[t_l, t_l + U(x_l)]$ must be all released out during $[t_l + U(x_l), t_{l+1}]$:

$$\int_{t_l}^{t_l + U(x_l)} g_i^s(t) dt = \int_{t_l + U(x_l)}^{t_{l+1}} g_i^r(t) dt \qquad (6)$$

A maximum data releasing rate g_{max} is set to keep interfered sensors in N_l from releasing their stored data with extremely high transmission rate simultaneously, since it might lead to frequent medium access collisions. Namely,

$$0 \leq g_i^r(t) \leq g_{max} \qquad (7)$$

Regulating $g_i^r(t)$ will largely decrease the collision possibilities, though can not thoroughly avoid it. Then, the remained collisions can be handled by collision resolution protocols [23].

E. Energy Profiles

Recent studies [19] [22] discussed the situation that the recharged energy is infinite and the sensor network stays operational forever. In this paper, we focus on a different scenario where the total amount of energy assigned for the network is limited to E [24]. Specifically, E equals to the sum of sensors' initial battery and recharged energy.

In practice, a typical sensor network's life span is consisted of deployment, initial and operational intervals. During the deployment interval (before $t = 0$), sensors are fairly allocated with the same amount of initial battery h_0 and randomly distributed to the interested area. Denote the initial interval as $[0, T_0]$, during which initial operations such as neighbor discovery and routing construction are performed. Meantime, the charger visits each sensor once and charges its battery to an appropriate level to support monitoring operations during the next interval. Denote the charging duration for sensor i as τ_i and the traveling time to visit all sensors as t_{TL}, then, we have:

$$T_0 = t_{TL} + \sum_{i \in N} \tau_i$$

During the initial interval, denote the energy charging rate as ϖ_0, each sensor consumes energy with a rate of e_0 and sensor i's battery status at $t = T_0$ is H_i. Then, we have:

$$H_i = \varpi_0 \tau_i + h_0 - e_0 T_0, \quad \forall i \in N$$

Denote T_1 as the end time of the sensor network, which is defined as the first time a sensor runs out of energy. During operational interval $[T_0, T_1]$, sensors monitor the interested

environment and forward sensory data to the sink. The network lifetime T is defined as the duration of operational interval, namely, $T = T_1 - T_0$. Because data transmissions are more important than initial interactions, during the operational interval, energy should be transferred more cautiously to avoid large scale interference. Thus we have $\varpi < \varpi_0$, where ϖ and ϖ_0 are energy charging rates during operational and initial intervals, respectively.

For sensor i, denote e_{il} the energy consumption during $[t_l, t_{l+1}]$. Then, we have:

$$e_{il} = \int_{t_l}^{t_{l+1}} e_i(t)dt$$

Denote $B_i(t_l)$ the battery status of sensor i at time t_l, to guarantee each sensor never runs out of energy before T_1, the following energy constraint must be satisfied:

$$B_i(t_l) = H_i - \sum_{\epsilon=0}^{l}(e_{i\epsilon} - K_{i\epsilon}) \geq 0, \quad i \in N, l \in L \tag{8}$$

Since the total energy that can be assigned to the sensor network is limited to E, we have the following constraint:

$$Nh_0 + \varpi_0 \sum_{i \in N} \tau_i + \varpi \sum_{l \in L} U(x_l) \leq E \tag{9}$$

where Nh_0, $\varpi_0 \sum_{i \in N} \tau_i$ and $\varpi \sum_{l \in L} U(x_l)$ are total energy allocated/recharged during deployment, initial and operational intervals, respectively.

IV. Problem Formulation

In this section, we first formulate the lifetime maximization problem as a time-dependent continuous problem(*OR-C*). Due to its high complexity, next, we convert it to a time-independent discrete problem(*OR-D*) and prove that problem(*OR-D*) achieves the same maximum network lifetime as problem(*OR-C*). Though problem(*OR-D*) is also NP-hard, near optimal solutions can be constructed on its basis.

A. Continuous Formulation

Since the charger sojourns and travels within the network area during the whole operational interval, network lifetime T equals to the sum of the charger's sojourn and traveling durations during $[T_0, T_1]$ [6]. Thus the lifetime maximization problem can be formulated as:

$$\begin{aligned} \max \quad & T = \sum_{l \in L}[U(x_l) + U(y_l)] \qquad \text{(OR-C)} \\ \text{s.t.} \quad & \text{Eq. } (3) - (9) \end{aligned}$$

In the above formulation, Eq. (3) (5) are flow conservation constraints, Eq. (4) avoids the stored data occupy excessive storage, Eq. (6) ensures all stored data are released from sensors' storage, Eq. (7) tries to mitigate medium access collisions, Eq. (8) ensures that sensors never run out of energy before T_1, and Eq. (9) regulates that the total amount of energy assigned to the network is finite.

Problem(*OR-C*) is highly complicated and can not be solved in polynomial time due to the following reasons:

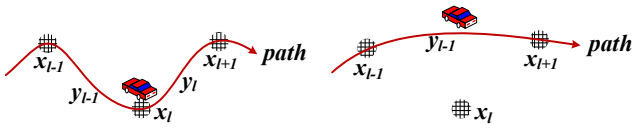

(a) Case 1 & 2. (b) Case 3.

Fig. 3. An illustrative example of different charger behaviors.

- In terms of flow routing, $g_{ij}(t)$, $g_{i0}(t)$, $g_i^s(t)$ and $g_i^r(t)$ are all continuous functions of time t. There can be infinite number of t, thus infinite number of possible value of data flow functions. Hence, problem(*OR-C*) is in the form of non-polynomial programming.
- The charger's visit sequence L is unknown, which can be determined after a traveling path of the charger is found. However, finding the charger's optimal traveling path is NP-hard. Considering the simplest path planning problem, TSP, is generally NP-hard.

Before a near optimal solution can be constructed, we convert the time-dependent continuous problem(*OR-C*) to a time-independent discrete problem(*OR-D*) borrows idea from Shi *et al.* [18]. Note that in [18], the authors only considered the static situation, where the sensor network did not operate when the charger was traveling, which differs from our model that the sensor network operates continuously during its whole lifetime. Moreover, in our model, network circumstances, sensor and charger behaviors are different from [18].

B. Discrete Formulation

Actually, different relations between $U(x_l)$ and $U(\nu_l)$ reflect the charger's different behaviors. In particular, there exists three different charger behaviors [1].

- Case 1: $U(x_l) > 0$ and $U(y_l) > 0$. The charger sojourns at x_l for duration $U(x_l)$ and spends $U(y_l)$ to traverse y_l.
- Case 2: $U(x_l) = 0$ and $U(y_l) > 0$. The charger passes x_l without sojourn and spends $U(y_l)$ to traverse y_l.
- Case 3: $U(x_l) = U(y_l) = 0$. The charger directly sets out for location x_{l+1} after x_{l-1} is visited.

An example of different charger behaviors is shown in Fig. 3. To formulate a time-independent discrete optimization, we define time-independent data flow functions as the average of their time-dependent counterparts. As to case 1, for sensor i during $[t_l, t_l + U(x_l)]$, we have:

$$\text{Sensor } i \text{ to sensor } j: \quad f_{ij}(x_l) = \frac{\int_{t_l}^{t_l+U(x_l)} g_{ij}(t)dt}{U(x_l)}$$

$$\text{Sensor } i \text{ to the sink:} \quad f_{i0}(x_l) = \frac{\int_{t_l}^{t_l+U(x_l)} g_{i0}(t)dt}{U(x_l)}$$

$$\text{Sensor } i \text{ stores data:} \quad f_i^s(x_l) = \frac{\int_{t_l}^{t_l+U(x_l)} g_i^s(t)dt}{U(x_l)}$$

[1] In section V, we will show that the case $U(x_l) > 0$ and $U(y_l) \leq 0$ is nonexistent based on theorem 2.

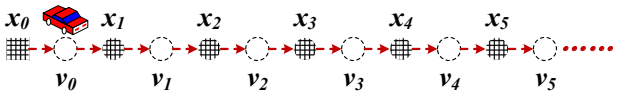

Fig. 4. Replace the time-dependent continuous path segment y_l with time-independent discrete virtual point ν_l. Then, the charger's traveling path is consisted of discrete points x_l and ν_l.

In the discrete formulation, the time-dependent continuous path segment y_l is replaced with the time-independent discrete virtual point ν_l (see Fig. 4). Let $U(\nu_l) = U(y_l)$, then, data flow functions during $[t_l + U(x_l), t_{l+1}]$ can be transformed as follows:

$$\text{Sensor } i \text{ to sensor } j: \quad f_{ij}(\nu_l) = \frac{\int_{t_l+U(x_l)}^{t_{l+1}} g_{ij}(t)dt}{U(\nu_l)}$$

$$\text{Sensor } i \text{ to the sink:} \quad f_{i0}(\nu_l) = \frac{\int_{t_l+U(x_l)}^{t_{l+1}} g_{i0}(t)dt}{U(\nu_l)}$$

$$\text{Sensor } i \text{ releases data:} \quad f_i^r(\nu_l) = \frac{\int_{t_l+U(x_l)}^{t_{l+1}} g_i^r(t)dt}{U(\nu_l)}$$

With regard to case 2, we define $f_{ij}(x_l) = g_{ij}(t_l)$, $f_{i0}(x_l) = g_{i0}(t_l)$ and $f_i^s(x_l) = g_i^s(t_l)$. Data flow functions during $[t_l + U(x_l), t_{l+1}]$ are transformed similar to case 1. As to case 3, we define $f_{ij}(x_l) = g_{ij}(t_l)$, $f_{i0}(x_l) = g_{i0}(t_l)$, $f_i^s(x_l) = g_i^s(t_l)$, $f_{ij}(\nu_l) = g_{ij}(t_l)$, $f_{i0}(\nu_l) = g_{i0}(t_l)$ and $f_i^r(\nu_l) = g_i^r(t_l)$.

In the discrete formulation, for sensor i, when the charger sojourns at x_l and ν_l, flow conservation equations are:

$$\sum_{k\in N}^{k\neq i} f_{ki}(x_l) + g_i = \sum_{j\in N}^{j\neq i} f_{ij}(x_l) + f_{i0}(x_l) + f_i^s(x_l) \tag{10}$$

and

$$\sum_{k\in N}^{k\neq i} f_{ki}(\nu_l) + g_i = \sum_{j\in N}^{j\neq i} f_{ij}(\nu_l) + f_{i0}(\nu_l) - f_i^r(\nu_l) \tag{11}$$

For sensor $i \notin N_l$, data communications are not interfered, such that $f_i^s(x_l) = 0$. As to interfered sensor $i \in N_l$, data should be stored to avoid loss, thus $f_i^s(x_l) = g_i$. As we discussed before, data stored during $[t_l, t_l + U(x_l)]$ should be all released out during $[t_l + U(x_l), t_{l+1}]$ to avoid long delay:

$$f_i^s(x_l)U(x_l) = f_i^r(\nu_l)U(\nu_l) \tag{12}$$

Similar to the time-dependent situation, data releasing rate should be restricted to avoid medium access collisions, namely:

$$0 \leq f_i^r(\nu_l) \leq g_{max} \tag{13}$$

Energy consumption rates for sensor i during $[t_l, t_l+U(x_l)]$ and $[t_l + U(x_l), t_{l+1}]$ are converted as follows:

$$e_i(x_l) = \sum_{k\in N}^{k\neq i} \rho f_{ki}(x_l) + \sum_{j\in N}^{j\neq i} C_{ij} f_{ij}(x_l) + C_{i0} f_{i0}(x_l)$$

and

$$e_i(\nu_l) = \sum_{k\in N}^{k\neq i} \rho f_{ki}(\nu_l) + \sum_{j\in N}^{j\neq i} C_{ij} f_{ij}(\nu_l) + C_{i0} f_{i0}(\nu_l)$$

Energy consumed during $[t_l, t_{l+1}]$ is $e_{il} = e_i(x_l)U(x_l) + e_i(\nu_l)U(\nu_l)$.

Then, the time-independent discrete problem(*OR-D*) can be formulated as follows:

$$\begin{aligned} \max \quad & T = \sum_{l\in L} [U(x_l) + U(\nu_l)] \\ \text{s.t.} \quad & \text{Eq. } (4), (8) - (13) \end{aligned} \tag{OR-D}$$

The following theorem shows that it is feasible to obtain the maximum network lifetime of the original problem(*OR-C*) by solving problem(*OR-D*).

Theorem 1. *The optimal solution of problem(OR-D) can achieve the same maximum network lifetime as problem(OR-C).*

We refer the readers to appendix A for a comprehensive proof.

V. A Near Optimal Solution

This section is organized as follows: In section V-A, we discuss the minimum energy routing. Next, we build a linear programming with relaxed energy constraint to approximate the original problem(*OR-D*). Based on this relaxed problem, a near optimal solution is constructed in section V-C. Finally, we give a summary of our solution in section V-D.

A. Minimum Energy Routing

In this paper, minimum energy routing is defined as the routing scheme of a sensor network that achieves the minimum total energy consumption.

1) Basic Network Model: To prolong the network lifetime, naturally, data should be forwarded to the sink in an energy-efficient way. The minimum energy routing in the basic model (section III-A) can be calculated by the following linear programming:

$$\begin{aligned} \min \quad & \sum_{i\in N} e_i(t) \\ \text{s.t.} \quad & \text{Eq. } (1), (2) \end{aligned} \tag{MIN-B}$$

Problem(*MIN-B*) can be easily solved by optimization tools such as CPLEX [8]. Suppose η_i is the resulted energy consumption rate of sensor i, then the minimum total energy consumption rate is $\sum_{i\in N} \eta_i$.

2) Extended Network Model: In regard to the extended model with a mobile charger, the minimum energy routing during $[t_l, t_{l+1}]$ can be calculated by the following optimization:

$$\begin{aligned} \min \quad & \sum_{i\in N} [e_i(x_l)U(x_l) + e_i(\nu_l)U(\nu_l)] \\ \text{s.t.} \quad & \text{Eq. } (10) - (13), \quad U(x_l) = 1 \end{aligned} \tag{MIN-E}$$

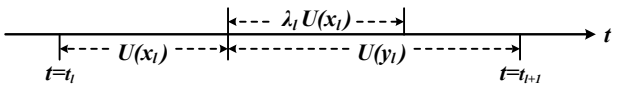

Fig. 5. Relations between $U(x_l)$ and $U(\nu_l)$.

Since the duration $[t_l, t_{l+1}]$ is unknown yet, the charger's sojourn duration $U(x_l)$ is set to a unit of time, and constraints Eq. (4) (8) (9) are temporarily neglected. Problem(*MIN-E*) is a quadratic programming due to the quadratic term $e_i(\nu_l)U(\nu_l)$. Before we can solve it, the following theorem is given to convert it to a linear programming.

Theorem 2. *For a given $U(x_l) > 0$, denote g^l_{max} the maximum data generation rate for all interfered sensors. Namely, $g^l_{max} = max(g_i)$, $i \in N_l$. To obtain the minimum energy routing during $[t_l, t_{l+1}]$, $U(\nu_l) = \lambda_l U(x_l)$ must hold, where*

$$\lambda_l = \frac{g^l_{max}}{g_{max}} > 0$$

Note that g_{max} is the maximum data releasing rate. We refer the readers to appendix B for a comprehensive proof.

Based on the above theorem, problem(*MIN-E*) can be converted to a linear programming solved by CPLEX. Suppose the resulted energy consumptions of sensor i during $[t_l, t_l+U(x_l)]$ and $[t_l + U(x_l), t_{l+1}]$ are ε_{il} and μ_{il}, respectively. Then, the minimum total energy consumption during $[t_l, t_{l+1}]$ is $\sum_{i\in N}[\varepsilon_{il}U(x_l) + \mu_{il}U(\nu_l)]$.

3) Minimum Energy Routing and Charger Behaviors: As we mentioned before, charger behaviors can be reflected by the relation between $U(x_l)$ and $U(\nu_l)$, which also affects the minimum energy routing. Take Fig. 5 as an example, if $U(x_l) = 0$ and $U(\nu_l) > 0$, sensors only need to forward newly generated data during $[t_l+U(x_l), t_{l+1}]$. However, if $U(x_l) > 0$ and $U(\nu_l) > 0$, sensors are required to forward both stored and newly generated data during $[t_l+U(x_l), t_{l+1}]$. Since we can not predict the values of $U(x_l)$ and $U(\nu_l)$, each relation should be considered carefully. In particular, four possible relations are listed below:

- Relation 1: $U(x_l) > 0$ and $U(\nu_l) > \lambda_l U(x_l)$
- Relation 2: $U(x_l) > 0$ and $U(\nu_l) = \lambda_l U(x_l)$
- Relation 3: $U(x_l) = 0$ and $U(\nu_l) > 0$
- Relation 4: $U(x_l) = 0$ and $U(\nu_l) = 0$

Based on results obtained from problem(*MIN-B*) and (*MIN-E*), we give the following proposition to calculate sensor i's energy consumption during $[t_l, t_{l+1}]$ regardless of the relation between $U(x_l)$ and $U(\nu_l)$.

Proposition 1. *Suppose the minimum energy routing is always adopted during the operational interval $[T_0, T_1]$, then the energy consumption of sensor i during $[t_l, t_{l+1}]$ can be calculated by:*

$$e_{il} = \varepsilon_{il}U(x_l) + \mu_{il}\lambda_l U(x_l) + [U(\nu_l) - \lambda_l U(x_l)]\eta_i$$

We refer the readers to appendix C for a comprehensive proof.

B. Problem Relaxation

Charger scheduling includes finding the charger's optimal traveling path consists of x_l and ν_l, and deciding durations $U(x_l)$ and $U(\nu_l)$. To construct a near optimal solution to the original problem(*OR-D*), we temporarily neglect the maximum sojourn time constraint Eq. (4) and relax the energy constraint Eq. (8). Then, a relaxed problem can be built as follows:

$$\max \quad T = \sum_{l\in L}[U(x_l) + U(\nu_l)] \tag{RLX}$$
$$\text{s.t.} \quad \text{Eq. } (9) - (13)$$
$$B_i(T_1) = H_i - \sum_{l\in L}(e_{il} - K_{il}) = 0, \quad \forall i \in N \tag{14}$$

Note that constraint Eq. (14) in problem(*RLX*) is a relaxed edition of constraint Eq. (8) in the original problem(*OR-D*).

To reduce the complexity of problem(*RLX*), we simplify the charger's traveling path to a single TSP path. Further, we suppose the minimum energy routing is adopted during the whole operational interval $[T_0, T_1]$, then a linear programming can be constructed follows:

$$\max \quad T = \sum_{l\in L}[U(x_l) + U(\nu_l)] \tag{LP-T}$$
$$\text{s.t.} \quad \text{Eq. } (9), \quad L = N$$
$$U(\nu_l) \geq \lambda_l U(x_l), \quad \forall l \in L \tag{15}$$
$$\sum_{l\in L} e_{il} - \varpi U(x_i) = H_i, \quad \forall i \in N \tag{16}$$

Note that $L = N$ stands for the fact that the charger's traveling path is a single TSP path. Due to the adoption of minimum energy routing, constraint Eq. (14) is equivalently transformed to Eq. (16). Details are omitted to conserve space.

The following theorem shows that it is sufficient to solve problem(*LP-T*) for the objective of lifetime maximization in problem(*RLX*).

Theorem 3. *The optimal solution of problem(LP-T) is also the optimal solution of problem(RLX).*

We refer the readers to appendix D for a comprehensive proof.

C. Satisfying All Constraints

Based on theorem 3, the optimal solution of problem(*RLX*) can be obtained by solving linear programming problem(*LP-T*). However, comparing to the original problem(*OR-D*), problem (*RLX*) lacks of two constraints: sojourn time constraint Eq. (4) and energy constraint Eq. (8). In this part, we will show the way to construct a near optimal solution of problem(*OR-D*) that meets all constraints.

1) Sojourn Time Constraint Eq. (4): To construct a solution that satisfies the sojourn time constraint, the single TSP path is divided into W repeated TSP paths, where W is an arbitrary positive integer. During each TSP path, sojourn time $U(x_l)$ is reduced by $\frac{1}{W}$. Eq. (4) can be satisfied only if W is large

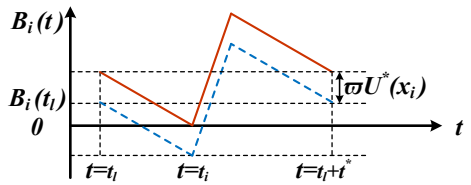

Fig. 6. Satisfying energy constraint Eq. (8) by assigning sensor i with additional energy $\varpi U^*(x_i)$.

enough. We construct the following linear programming:

$$\max \quad T = W \sum_{l \in N} [U(x_l) + U(\nu_l)] \tag{LP-W}$$

$$\text{s.t.} \quad \text{Eq. (15)}, \quad L = N$$

$$\sum_{l \in L} e_{il} - \varpi U(x_i) = \frac{H_i}{W}, \quad \forall i \in N \tag{17}$$

$$Nh_0 + \varpi_0 \sum_{i \in N} \tau_i + W\varpi \sum_{l \in L} U(x_l) \leq E \tag{18}$$

The following theorem shows that we can set arbitrary W, while the maximize lifetime T will remain uninfluenced.

Theorem 4. *Suppose P^* is the optimal solution of problem (LP-T) with the maximum network lifetime T^*. Then, T^* can be achieved by problem(LP-W) regardless of W.*

We refer the readers to appendix E for a comprehensive proof.

Similar to theorem 4, we can prove that if $U(x_l)$ and $U(\nu_l)$ are optimal results of problem(*LP-T*), then, $\frac{U(x_l)}{W}$ and $\frac{U(\nu_l)}{W}$ are optimal results of problem(*LP-W*). The network lifetime T is irrelevant to W, however, the value of W will decide whether the sojourn time constraint is satisfied. Suppose the optimal sojourn time obtained by solving problem(*LP-T*) is $U^t(x_l)$. Then, the maximum sojourn time in problem(*LP-W*) must be shorter than U_{max}. Namely,

$$max(\frac{U^t(x_l)}{W}) \leq U_{max}$$

Thus we have

$$W \geq \frac{max(U^t(x_l))}{U_{max}}, \quad W \in Z^+$$

When the above inequality holds, the solution of problem(*LP-W*) will satisfy the sojourn time constraint Eq. (4).

2) Energy Constraint Eq. (8): We focus on one of the W repeated TSP paths. Suppose the optimal solution of problem(*LP-W*) consists of e^*_{il}, $U^*(x_l)$ and $U^*(\nu_l)$, and that t^* is the time required to finish one TSP path. Based on Eq. (17), during one TSP path, sensor i's energy consumption comes from two sources: sensor i's initial battery $\frac{H_i}{W}$ and energy replenished by the charger, i.e., $\varpi U^*(x_i)$.

Before the charger visits and recharges sensor i, energy from sensor i's initial battery may be depleted. Namely, $\frac{H_i}{W} \leq \sum_{l \in N} e^*_{il}$. Thus the energy constraint Eq. (8) is violated. Take the dash line in Fig. 6 as an example. At time t_l, the charger is sojourning at x_l and the energy remained in sensor i's battery is $B_i(t_l)$. Before the charger arrives at sensor i at $t = t_i$, its battery depletes and the energy constraint is violated. To avoid it, as the solid line shown in Fig. 6, we only need to assign sensor i with additional energy $\varpi U^*(x_i)$. Suppose each sensor is assigned with an additional energy ζ, thus we have

$$\zeta = max(\varpi U^*(x_i)), \quad \forall i \in N \tag{19}$$

The total amount of additional energy $N\zeta$ can not be allocated directly from E since energy allocations are determined after we solve problem(*LP-W*). However, we can cancel the last $\phi \in Z^+$ TSP paths and assign the reserved energy carried by the charger. The reserved energy should be large enough to guarantee each sensor is assigned with energy ζ during initial interval, thus we have:

$$\phi\varpi \sum_{i \in N} U^*(x_i) \geq N\zeta(1 + \frac{Ne_0}{\varpi_0})$$

where the left part is the reversed energy, $N\zeta$ is the total required additional energy, and $N\zeta\frac{Ne_0}{\varpi_0}$ is the energy consumed to assign $N\zeta$. Then, we can obtain:

$$\phi \geq \frac{N\zeta(Ne_0 + \varpi_0)}{\varpi\varpi_0 \sum_{i \in N} U^*(x_i)}$$

where ϕ is irrelevant to W.

D. Solution Summary

Now, we give a summary of our near optimal solution:

(1) Let $L = N$, for each sojourn location x_l ($l \in N$), calculate N^*_l and λ^*_l.

(2) Next, solve problem(*MIN-B*) and (*MIN-E*) to obtain minimum energy routing. For each sensor $i \in N$, calculate η^*_i, ε^*_{il} and μ^*_{il}.

(3) Based on η^*_i, ε^*_{il} and μ^*_{il}, solve problem(*LP-T*). The optimal solution consists of $U^t(x_l)$, $U^t(\nu_l)$, τ^t_i and $T^t = \sum_{l \in N}[U^t(x_l) + U^t(\nu_l)]$. Note that T^t is an upper bound of the proposed near optimal solution since it is the optimal solution of the relaxed problem(*RLX*).

(4) Solve problem(*LP-W*), obtain optimal results $U^*(x_l)$ and $U^*(\nu_l)$. Set $W^* = \lceil \frac{max(U^t(x_l))}{U_{max}} \rceil$, $\zeta^* = max(\varpi U^*(x_i))$ and $\phi^* = \lceil \frac{N\zeta^*(Ne_0 + \varpi_0)}{\varpi\varpi_0 \sum_{i \in N} U^*(x_i)} \rceil$.

(5) Finally, the near optimal solution of the original problem(*OR*) are constructed as follows: (i) Let $\tau^* = \tau^t_i + \frac{\zeta^*}{\varpi_0}$, during initial interval, the charger charges each sensor, say i, with energy of $\varpi_0\tau^*_i$. (ii) Adopt minimum energy routing during the whole network lifetime. Specifically, during $[t_l, t_l + \lambda_l U^*(x_l)]$ and $[t_l + \lambda_l U^*(x_l), t_{l+1}]$, adopt minimum energy routings obtained from problem(*MIN-E*) and (*MIN-B*), respectively. (iii) Solve problem(*LP-W*) and the charger travels $W^* - \phi^*$ repeated TSP paths. Thus, the near optimal network lifetime $T^* = (W^* - \phi^*) \sum_{l \in N}[U^*(x_l) + U^*(\nu_l)]$.

Since T^t is an upper bound of T^*, the optimality of our near optimal solution is:

$$\frac{T^*}{T^t} = \frac{(W^* - \phi^*) \sum_{l \in N}[U^*(x_l) + U^*(\nu_l)]}{\sum_{l \in N}[U^t(x_l) + U^t(\nu_l)]} = 1 - \frac{\phi^*}{W^*}$$

TABLE I
A NUMERICAL EXAMPLE: SOLUTION DETAILS

Variables	Sensor Index (i)														
	1	2	3	4	5	6	7	8	9	10	11	12	13	14	15
x-$axis$	91	171	63	14	37	131	92	118	100	177	11	32	177	34	194
y-$axis$	80	186	86	40	146	159	22	165	23	70	66	179	115	107	95
g_i	5	2	6	3	3	6	4	3	7	8	4	4	1	8	2
λ_i	0.60	0.60	0.80	0.40	0.80	0.60	0.70	0.60	0.70	0.80	0.80	0.40	0.80	0.80	0.80
τ_i	3	3	3	2.32E4	3	3	3	3	3	3	2.04E4	3	3	7.22E3	3
H_i	951	951	951	2.41E4	951	951	951	951	951	951	2.14E4	951	951	8.17E3	951
$U(x_i)$	44.7	0.68	23.6	0	8.86	17.1	60	19.5	31.2	40.5	0	5.87	1.17	0	0.59
$U(\nu_i)$	839	0.41	18.9	0	7.09	10.2	42	11.7	21.9	32.4	0	2.34	0.93	0	0.47

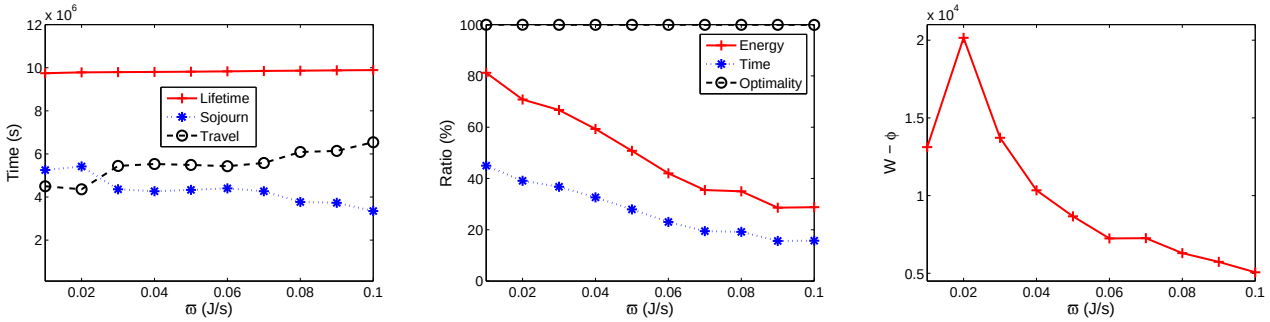

(a) Network lifetime details. (b) Allocation ratio during T_0 and optimality. (c) Number of repeated TSP paths.

Fig. 7. Parameter analysis of charging rate ϖ.

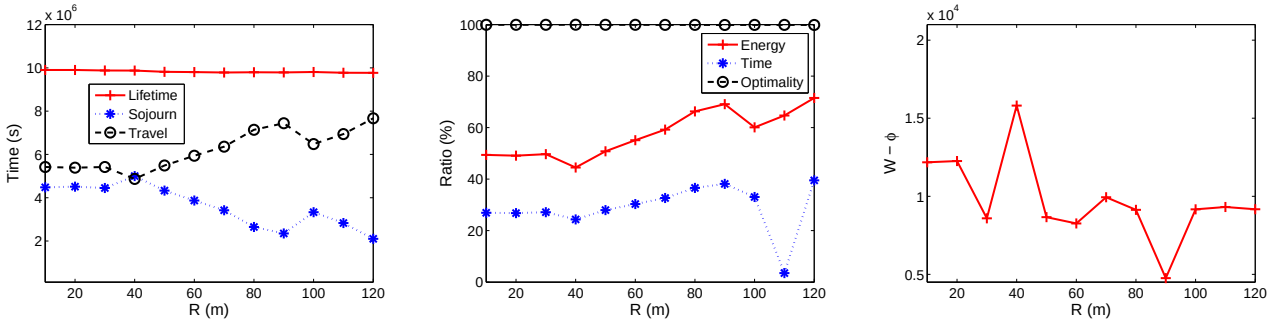

(a) Network lifetime details. (b) Allocation ratio during T_0 and optimality. (c) Number of repeated TSP paths.

Fig. 8. Parameter analysis of interference radius R.

VI. EVALUATION

In this section, we first give a numerical example to present some interesting results of our solution. Then, we extensively evaluate it under different parameter settings and reveal insights of the solution performance. Finally, we give some comparisons to show the effectiveness of the proposed solution.

We assume that sensors are randomly distributed over a $200m * 200m$ two-dimensional square area, the sink is located at (0, 0), and sensors' data generation rate are randomly generated within $[1, 10]$ kb/s. Energy consumption coefficients $\beta_1 = 50$ nJ/b, $\beta_2 = 0.0013$ pJ/$(b \cdot m^4)$, $\alpha = 4$ and $\rho = 50$ nJ/b. The charger sojourns at the sink when $t = 0$. Energy charging rates during initial and operational intervals are $\varpi_0 = 1$ J/s and $\varpi = 0.05$ J/s, respectively. The charging interference radius is $R = 50$ m.

We assume that the total energy E is proportional to the number of sensors, namely, $E = N \times 10^4$ J. The beginning battery is set to $h_0 = 1000$ J and the energy consumption rate during initial interval is $e_0 = 1 \times 10^{-3}$ J/s. Moreover, the maximum sojourn time is $U_{max} = 60$ s, the maximum data releasing rate is $g_{max} = 10$ kb/s, and the charger's traveling time during initial interval is $t_{TL} = 1000$ s.

A. A Numerical Example

To give an illustrative example, we build a 15-sensor random network with initial energy $h_0 = 100$ J. Here, h_0 is set to a small value to accommodate the small network. Following default settings, we run the solution and obtain optimal network lifetime $T = 9.4 \times 10^6$ s. Details are listed in Table I, where (*x-axis*, *y-axis*) represents sensor locations. Based on step (4) of our solution, $W = 7580$ and $\phi = 4$. Thus the network terminates after the charger repeats $W - \phi = 7576$

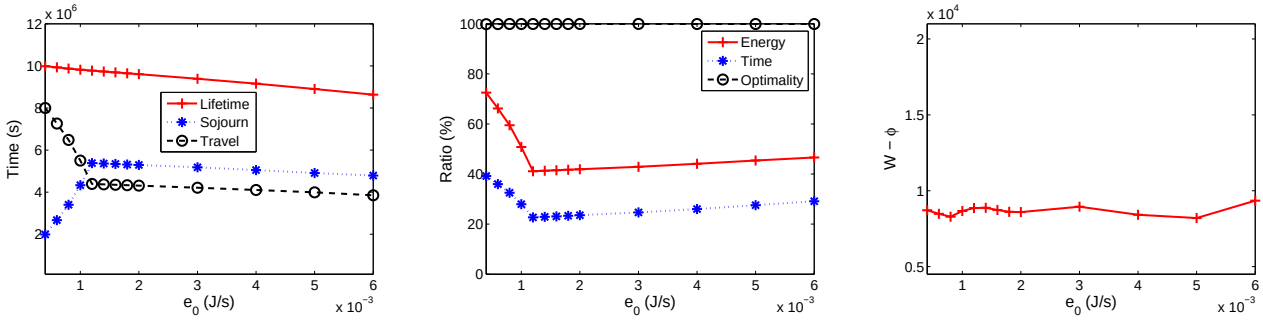

(a) Network lifetime details. (b) Allocation ratio during T_0 and optimality. (c) Number of repeated TSP paths.

Fig. 9. Parameter analysis of initial energy consumption rate e_0.

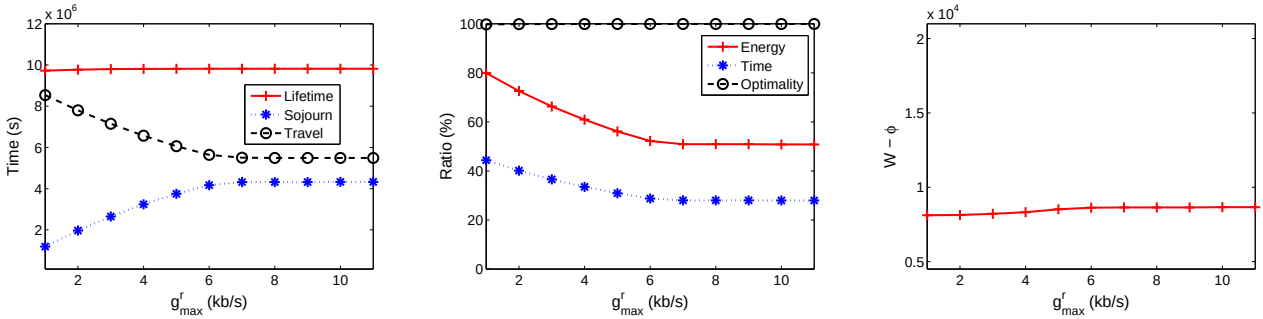

(a) Network lifetime details. (b) Allocation ratio during T_0 and optimality. (c) Number of repeated TSP paths.

Fig. 10. Parameter analysis of the maximum data releasing rate g_{max}.

TSP paths. In this case, the optimality of our near optimal solution is $1 - \frac{\phi}{W} = 99.95\%$.

B. Parameter Analysis

In this part, we increase the number of sensors to 50 and analyze how the parameter settings influence our solution. Two parameters are considered here: energy charging rate ϖ, interference radius R, energy consumption rate during initial interval e_0, and the maximum data releasing rate g_{max}. For each parameter, we care about the following solution details: network lifetime T, energy allocated during initial/operational intervals, solution optimality, and the number of repeated TSP paths.

To analyze ϖ, we vary it from 0.01 J/s to 0.1 J/s while keeping other parameters unchanged. From Fig. 7(a), we find that ϖ has limited influence to T. However, it affects the constituent parts of T: sojourn and traveling time. With larger ϖ, the charger spends less time on energy transfer (sojourn), but more time on traveling. Impressively, as shown in Fig. 7(b), the near optimal solution always achieves above 99% optimality. The high optimality is obtained by jointly optimizing data transmission and charger scheduling.

Moreover, ϖ has direct influences on energy allocation. Since the initial battery h_0 is constant, here we focus on energy allocation ratio during initial interval, i.e., $\frac{\sum_{i \in N} \varpi_0 \tau_i}{E}$. In Fig. 7(b), when $\varpi = 0.01$ J/s, 81.2% of energy is allocated during $[0, T_0]$ while less than 10% energy is allocated during $[T_0, T_1]$. When ϖ increases to 0.1 J/s, above 60% energy is allocated during $[T_0, T_1]$ while only 28.8% is during $[0, T_0]$. The ratio $\frac{T_0}{T}$ follows the same trend.

Another factor we care about is the number of TSP paths, i.e., $W - \phi$. As shown in Fig. 7(c), as ϖ increases, $W - \phi$ increases first and after a threshold (here is $\varpi = 0.02$ J/s) is surpassed, $W - \phi$ decreases quickly. The incremental part is caused by the charger's frequent movement to transfer more energy. After $\varpi \geq 0.02$, the charger has stronger charging ability, and it could sojourn longer to achieve higher energy transfer. Thus $W - \phi$ decreases.

In terms of interference radius R, the network lifetime varies slowly (see Fig. 8(a)). Compared to ϖ, an apparent characteristic of R is the large randomness. Although T keeps stable, sojourn and traveling durations vary widely. With the increase of R, generally, the sojourn time decreases while the travel time increases. Since larger R causes more interfered sensors, the charger tends to sojourn less when R is large. The energy and time ratios both increase as R increases, also with random fluctuations (see Fig. 8(b)). In Fig. 8(c), the large randomness of $W - \phi$ is mainly caused by the sensor distribution. For example, when the charger is visiting sensor i with $R = 20$ m, 3 sensors around i may be interfered. However, this number may increase to 15 when $R = 40$ m due to the random distribution of sensors.

Different from ϖ and R, e_0 has significant effect on the network lifetime. As shown in Fig. 9(a), when e_0 increases, network lifetime decreases quickly. Specifically, when e_0 is very small (here is $e_0 < 1.2 \times 10^{-3}$ J/s), sojourn time increases while traveling time decreases with the increase of e_0. The reason here is apparently: larger e_0 leads to more energy consumption during initial interval. Thus T_0 is kept small and more energy is allocated during operational interval, leading

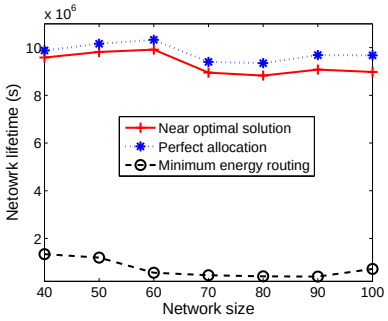

Fig. 11. Performance comparison: network lifetime.

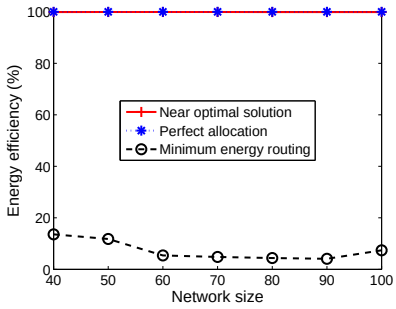

Fig. 12. Performance comparison: energy efficiency.

to larger sojourn time. After $e_0 > 1.2 \times 10^{-3}$ J/s, as the increase of e_0, sojourn and traveling time in Fig. 9(a) decrease while energy and time ratio in Fig. 9(b) increase, all in a linear manner. The decreased sojourn/travel times are caused by reduced network lifetime.

Reasons of increased energy/time ratios are more complex. To obtain longer network lifetime, sensors should be allocated with sufficient energy. Moreover, energy should be allocated among sensors in a balanced way. When e_0 surpassed a threshold (here is $e_0 > 1.2 \times 10^{-3}$ J/s), the energy balance becomes much more important than the energy quantity. Although larger e_0 leads to more energy consumption during initial interval, longer initial duration is still required to make energy allocations balanced. As to $W-\phi$ in Fig. 9(c), e_0 shows insignificant importance.

At last, we analyze the maximum data releasing rate g_{max}. As g_{max} increases, network lifetime and sojourn time increase while travel time decreases as shown in Fig. 10(a). When $g_{max} \in [1, 6]$ kb/s, sojourn and travel times vary quickly while after $g_{max} > 6$ kb/s, both vary slowly. Energy and time ratios in Fig. 10(b) present similar regularities. The same as e_0, g_{max} shows trivial importance to $W - \phi$.

C. Performance Comparison

In this paper, we set up two baselines to compare with our near optimal solution. The first one is minimum energy routing, which is pervasively adopted in practice. In this case, total energy E is averagely allocated among sensors. After deployment, sensors forward sensory data to the sink with a minimum energy routing. The second algorithm is named as perfect allocation. Suppose the minimum energy routing is adopted by the sensor network, total energy E is allocated based on the sensor energy consumption in a perfect way, which means that sensor batteries will be depleted simultaneously when the network terminates. We note that perfect allocation is unreachable in practice since we can not obtain sensor energy consumption information before energy is actually consumed. Perfect allocation represents the possible maximum network lifetime while the minimum energy routing stands for the generally adopted solution.

We vary the number of sensors from 40 to 100 to evaluate our solution in different network sizes. Impressively, as shown in Fig. 11, compared to the pervasively adopted minimum energy routing, our solution achieves 7.15 to 22.75 times longer network lifetime with the same amount of total energy E. Moreover, the ratio between our solution and the perfect allocation varies from 92.8% to 97%, which validates the high effectiveness. In terms of energy efficiency, as shown in Fig. 12, less than 0.2% energy is wasted by our solution. Compare to the perfect allocation, which utilized 100% energy, our solution presents very high efficiency. The minimum energy routing wastes above 86% energy. This is because the network lifetime is determined by the sensor with the largest energy consumption, when the network terminates, a large part of energy is remained in batteries of light-burdened sensors.

VII. Further Discussion

RF-WPT is known to be a promising way to solve energy bottlenecks for low power devices. Our study has provided evidences that RF-WPT chargers can be utilized to promote sensor network performances, even it introduces higher degree of interference. Considering that deploying mobile relays [16] [20] [17] in wireless sensor networks are mature technologies with years of exploration, implementing the proposed solution will not pose severer challenge. A simple and practical design is to make the charger a coordinator that controls sensor-charger collaboration [1] [12].

Our work remains an initial attempt toward jointly considering communication and charger scheduling in interference-aware environments. There are still many open issues that can be further explored, and we hereby list three in which we are particularly interested.

Sensor-charger interaction overheads: In our investigation, communications among sensors are optimized. However, in real environments, interactions between the charger and sensors are inevitable and lead to communication overheads. Efficient designs that minimize communication overheads are to be developed.

Sensor storage and charger traveling distance: Except for energy, storage is also very limited in sensors. To avoid large storage usage, in our solution, the charger sojourn time is restricted. This may cause frequent charger movements, leading to longer traveling distance. Therefore, tradeoffs between sensor storages and charger traveling distances are worth further exploitations.

Power transfer efficiency: In this study, we focus on allocating constant total energy E among sensors. To achieve this goal, in practice, more energy than E will be transferred by the charger due to efficiency problems. Although there has been

researches aiming at promoting power transfer efficiency[11] [3], more researches are still required.

VIII. Conclusion And Future Work

In this paper, we have investigated the joint optimization of maximizing network lifetime and avoiding data loss under charging interference concerns. Considering the complexity of the original problem, we have relaxed it and constructed a series of simpler optimizations. Based on them, a near optimal solution with provable $1-\frac{\phi}{W}$ performance guarantee has been developed. The effectiveness of our solution is validated with extensive evaluations and comparisons. In our future work, we will further explore the situation with very large scale networks and multiple mobile chargers.

References

[1] G. Anastasi, M. Conti, E. Monaldi, and A. Passarella. An adaptive data-transfer protocol for sensor networks with data mules. In *IEEE WoWMoM*, pages 1–8, 2007.

[2] W. C. Brown. The history of power transmission by radio waves. *IEEE Trans. Microwave Theory and Techniques*, 32(9):1230–1242, 1984.

[3] L. Chen, S. Liu, Y. C. Zhou, and T. J. Cui. An optimizable circuit structure for high-efficiency wireless power transfer. *IEEE Trans. Industrial Electronics*, 60(1):339–349, 2013.

[4] H. Dai, Y. Liu, G. Chen, X. Wu, and T. He. Safe charging for wireless power transfer. In *INFOCOM, 2014 Proceedings IEEE*, pages 1105–1113. IEEE, 2014.

[5] L. Fu, P. Cheng, Y. Gu, J. Chen, and T. He. Minimizing charging delay in wireless rechargeable sensor networks. In *IEEE INFOCOM*, pages 2922–2930, 2013.

[6] S. Guo, C. Wang, and Y. Yang. Mobile data gathering with wireless energy replenishment in rechargeable sensor networks. In *IEEE INFOCOM*, pages 1932–1940, 2013.

[7] S. He, J. Chen, F. Jiang, D. K. Yau, G. Xing, and Y. Sun. Energy provisioning in wireless rechargeable sensor networks. *IEEE Trans. Mobile Computing*, 12(10):1931–1942, 2013.

[8] IBM ILOG CPLEX Optimizer. http://www-01.ibm.com/software/integration/optimization/cplex-optimizer/.

[9] B. Kellogg, A. Parks, S. Gollakota, J. R. Smith, and D. Wetherall. Wi-fi backscatter: Internet connectivity for rf-powered devices. In *ACM SIGCOMM*, pages 607–618, 2014.

[10] A. Kurs, A. Karalis, R. Moffatt, J. D. Joannopoulos, P. Fisher, and M. Soljačić. Wireless power transfer via strongly coupled magnetic resonances. *Science*, 317(5834):83–86, 2007.

[11] S.-H. Lee and R. D. Lorenz. Development and validation of model for 95%-efficiency 220-w wireless power transfer over a 30-cm air gap. *IEEE Trans. Industry Applications*, 47(6):2495–2504, 2011.

[12] Z. Li, Y. Liu, M. Li, J. Wang, and Z. Cao. Exploiting ubiquitous data collection for mobile users in wireless sensor networks. *IEEE Trans. Parallel and Distributed Systems*, 24(2):312–326, 2013.

[13] V. Liu, A. Parks, V. Talla, S. Gollakota, D. Wetherall, and J. R. Smith. Ambient backscatter: wireless communication out of thin air. In *ACM SIGCOMM*, pages 39–50, 2013.

[14] M. Y. Naderi, K. R. Chowdhury, S. Basagni, W. Heinzelman, S. De, and S. Jana. Experimental study of concurrent data and wireless energy transfer for sensor networks. In *IEEE GLOBECOM*, 2014.

[15] M. Y. Naderi, K. R. Chowdhury, S. Basagni, W. Heinzelman, S. De, and S. Jana. Surviving wireless energy interference in rf-harvesting sensor networks: An empirical study. In *IEEE SECON*, 2014.

[16] U. Park and J. Heidemann. Data muling with mobile phones for sensornets. In *ACM Sensys*, pages 162–175, 2011.

[17] Y. Qu, K. Xu, J. Liu, and W. Chen. Towards a practical energy conservation mechanism with assistance of resourceful mules. *IEEE Internet of Things Journal*, 2(2):145–158, 2015.

[18] Y. Shi and Y. T. Hou. Some fundamental results on base station movement problem for wireless sensor networks. *IEEE/ACM Trans. Networking*, 20(4):1054–1067, 2012.

[19] Y. Shi, L. Xie, Y. T. Hou, and H. D. Sherali. On renewable sensor networks with wireless energy transfer. In *IEEE INFOCOM*, pages 1350–1358, 2011.

[20] A. A. Somasundara, A. Kansal, D. D. Jea, D. Estrin, and M. B. Srivastava. Controllably mobile infrastructure for low energy embedded networks. *IEEE Trans. Mobile Computing*, 5(8):958–973, 2006.

[21] L. Xie, Y. Shi, Y. T. Hou, and A. Lou. Wireless power transfer and applications to sensor networks. *IEEE Wireless Communications Magazine*, 20(4), 2013.

[22] L. Xie, Y. Shi, Y. T. Hou, W. Lou, H. D. Sherali, and S. F. Midkiff. Bundling mobile base station and wireless energy transfer: Modeling and optimization. In *IEEE INFOCOM*, pages 1636–1644, 2013.

[23] M. A. Yigitel, O. D. Incel, and C. Ersoy. QoS-aware MAC protocols for wireless sensor networks: A survey. *Elsevier Computer Networks*, 55(8):1982–2004, 2011.

[24] T. Zhu, Y. Gu, T. He, and Z.-L. Zhang. eshare: a capacitor-driven energy storage and sharing network for long-term operation. In *ACM Sensys*, pages 239–252, 2010.

Appendix A
Prove of Theorem 1

Proof: Suppose P is the optimal solution of problem(*OR-C*), which consists of the maximum network lifetime T, the optimal charger's traveling path, sojourn/traveling durations $U(x_l)$ and $U(y_l)$, and data flow functions $g_{ij}(t)$, $g_{i0}(t)$, $g_i^s(t)$ and $g_i^r(t)$. Based on solution P, we can constructed a solution P^* with lifetime T^* as follows. First, we keep the charger's traveling path and sojourn/traveling durations the same as solution P, then we can show that both solutions achieve the same network lifetime:

$$T^* = \sum_{l\in L}[U(x_l)+U(\nu_l)] = \sum_{l\in L}[U(x_l)+U(y_l)] = T$$

Next, we construct data flow functions of solution P^* as described in section IV-B. And we need to show that P^* is a feasible solution of problem(*OR-D*). Specifically, we need to prove that solution P^* meets constraints Eq. (4), (8)-(13). Here, we focus on constraints Eq. (10) and (11). The proofs are based on 3 different cases described in section IV-B.

Consider Eq. (11) in case 1, for sensor i, we have:

$$\begin{aligned}
&\sum_{k\in N}^{k\neq i} f_{ki}(\nu_l) + g_i \\
&= \sum_{k\in N}^{k\neq i} \frac{\int_{t_l+U(x_l)}^{t_{l+1}} g_{ki}(t)dt}{U(\nu_l)} + \frac{\int_{t_l+U(x_l)}^{t_{l+1}} g_i dt}{U(\nu_l)} \\
&= \frac{\int_{t_l+U(x_l)}^{t_{l+1}} [\sum_{k\in N}^{k\neq i} g_{ki}(t) + g_i]dt}{U(\nu_l)} \\
&= \frac{\int_{t_l+U(x_l)}^{t_{l+1}} [\sum_{j\in N}^{j\neq i} g_{ij}(t) + g_{i0}(t) + g_i^s(t)]dt}{U(\nu_l)} \\
&= \sum_{j\in N}^{j\neq i} f_{ij}(\nu_l) + f_{i0}(\nu_l) + f_i^s(\nu_l)
\end{aligned}$$

Constraint Eq. (10) in case 1 and Eq. (11) in case 2 can be proved in the same way. As to Eq. (10) in case 2, it can be

proved as follows:

$$\begin{aligned}\sum_{k\in N}^{k\neq i} f_{ki}(x_l) + g_i &= \sum_{k\in N}^{k\neq i} g_{ki}(t_l) + g_i \\ &= \sum_{j\in N}^{j\neq i} g_{ij}(t_l) + g_{i0}(t_l) + g_i^s(t_l) \\ &= \sum_{j\in N}^{j\neq i} f_{ij}(x_l) + f_{i0}(x_l) + f_i^s(x_l)\end{aligned}$$

As to case 3, both constraints Eq. (10) and (11) can be proved the same as Eq. (10) in case 2. The proofs for Eq. (4), (8), (9), (12) and (13) are very similar and are thus omitted to conserve space. Up to now, we have showed that all constraints of problem(*OR-D*) are met by solution P^*. Hence P^* is a feasible solution to problem(*OR-D*).

Finally, we need to show that P^* is the optimal solution of problem(*OR-D*). The proof is based on contradiction. Suppose $\overline{P}$ is the optimal solution of problem(*OR-D*) with the maximum network lifetime $\overline{T} > T$. Based on $\overline{P}$, we can construct a solution of problem(*OR-C*) with lifetime $\overline{T}$, which contradicts with the fact that T is the maximum network lifetime.

Since we have proved that $T^* = T$, the optimal solution of problem(*OR-D*) can achieve the same maximum network lifetime as problem(*OR-C*), which concludes the proof. ■

Appendix B
Proof of Theorem 2

The proof of Theorem 2 is based on the following lemmas.

Lemma 1. *For a given feasible charger traveling path and a sojourn point x_l, we have $U(\nu_l) \geq \lambda_l U(x_l)$.*

Proof: Since both g_{max}^l and g_{max} are positive parameters, $\lambda_l > 0$ holds. If $U(x_l) = 0$, $U(\nu_l) \geq \lambda_l U(x_l) = 0$ holds absolutely. Here, we emphasize on proving the $U(x_l) > 0$ case. Based on Eq. (10), we have $f_i^s(x_l) = g_i$. Together with Eq. (12) and (13), we can derive:

$$\begin{aligned}g_i U(x_l) &= f_i^s(x_l) U(x_l) \\ &= f_i^r(\nu_l) U(\nu_l) \leq g_{max} U(\nu_l)\end{aligned}$$

Hence, $g_{max}U(\nu_l) \geq g_i U(x_l)$ holds for all sensor in N_l. It absolutely holds for the sensor with maximum data generation rate in N_l, thus $g_{max}U(\nu_l) \geq g_{max}^l U(x_l)$, which concludes the proof. Note that this lemma also holds for the time-dependent continuous formulation, we omit the proof to conserve space. ■

Lemma 2. *Consider a data routing with full sensor participation, denote π_i the minimum energy consumption rate required to forward a unit of data from sensor i to the sink, and the corresponding routing path is F_i. Suppose each sensor has a unit of data generation rate, then, the combination of $\sum_{i\in N} F_i$ is the minimum energy routing with the minimum total energy consumption rate $\sum_{i\in N} \pi_i$.*

Proof: It is apparently that $\sum_{i\in N} F_i$ is a routing scheme of the sensor network. Next, we prove $\sum_{i\in N} F_i$ is the minimum energy routing using contradictions. Suppose M^* is a routing scheme that consumes less energy than $\sum_{i\in N} \pi_i$. Thus at least one routing path F_i^* in M^* consumes less energy than π_i, which contradicts with the fact that F_i is the minimum energy routing path. ■

Now, we begin to prove theorem 2.

Proof: During $[t_l + U(x_l), t_{l+1}]$, the sensory data generated by sensor i is consisted of two parts: $g_i^s(x_l)U(x_l)$ and $g_i U(\nu_l)$. The former is generated and stored during $[t_l, t_l + U(x_l)]$, and the latter is newly generated during $[t_l + U(x_l), t_{l+1}]$. Suppose the minimum energy routing is adopted during $[t_l, t_{l+1}]$, based on lemma 2, the total energy consumption during $[t_l + U(x_l), t_{l+1}]$ is:

$$\begin{aligned}&\sum_{i\in N} \pi_i [g_i^s(x_l)U(x_l) + g_i U(\nu_l)] \\ &= \sum_{i\in N} \pi_i g_i^s(x_l) U(x_l) + \sum_{i\in N} \pi_i g_i U(\nu_l) \\ &= \sum_{i\in N_l} \pi_i g_i U(x_l) + \sum_{i\in N} \pi_i g_i U(\nu_l) \\ &\geq \sum_{i\in N_l} \pi_i g_i U(x_l) + \sum_{i\in N} \pi_i g_i \lambda_l U(x_l)\end{aligned}$$

When $U(\nu_l) = \lambda_l U(x_l)$, the total energy consumption during $[t_l + U(x_l), t_{l+1}]$ is minimized, which concludes the proof. ■

Appendix C
Proof of Proposition 1

Proof: The proofs of relation 2 and 3 are apparently. After we solve problem(*MIN-E*), $e_{il} = \varepsilon_{il} U(x_l) + \mu_{il} U(\nu_l)$ can be easily obtained. Here, we focus on relation 1. We assume that the minimum energy routing during $[t_l, t_{l+1}]$ is unique (the proof of non-unique situation is similar). To prove the proposition, we only need to prove that the total energy consumption $\sum_{i\in N} e_{il}$ is minimal.

Based on lemma 2, we can derive $\sum_{i\in N} \eta_i = \sum_{i\in N} \pi_i g_i$ and

$$\sum_{i\in N} \mu_{il} \lambda_l U(x_l) = \sum_{i\in N_l} \pi_i g_i U(x_l) + \sum_{i\in N} \pi_i g_i \lambda_l U(x_l)$$

Then, we have:

$$\begin{aligned}&\sum_{i\in N} e_{il} \\ &= \sum_{i\in N} \varepsilon_{il} U(x_l) + \sum_{i\in N} \mu_{il} \lambda_l U(x_l) + \sum_{i\in N} [U(\nu_l) - \lambda_l U(x_l)] \eta_i \\ &= \sum_{i\in N} \varepsilon_{il} U(x_l) + \sum_{i\in N_l} \pi_i g_i U(x_l) + \sum_{i\in N} \pi_i g_i \lambda_l U(x_l) \\ &+ \sum_{i\in N} [U(\nu_l) - \lambda_l U(x_l)] \pi_i g_i \\ &= \sum_{i\in N} \varepsilon_{il} U(x_l) + \sum_{i\in N_l} \pi_i g_i U(x_l) + \sum_{i\in N} \pi_i g_i U(\nu_l)\end{aligned}$$

where $\sum_{i\in N} \varepsilon_{il} U(x_l)$ is the minimum energy consumption during $[t_l, t_l + U(x_l)]$ and the last two polynomials in the right part together represent the minimum energy routing during $[t_l + U(x_l), t_{l+1}]$, which concludes the proof. ■

APPENDIX D
PROOF OF THEOREM 3

The proof is based on the following lemmas.

Lemma 3. *A feasible solution of problem(LP-T) is also a feasible solution of problem(RLX).*

Proof: Suppose P is a feasible solution of problem(*LP-T*) that consists of $U(x_l)$ and $U(\nu_l)$. Since energy consumption results η_i, ε_{il} and μ_{il} are all obtained by solving problems(*MIN-B*) and (*MIN-E*), data routing constraints Eq. (10) - (13) are naturally satisfied by P. Let the charger travel a single TSP path (with each sensor visited once), constraint Eq. (16) is equivalent to constraint Eq. (14). Therefore, constraints Eq. (9)-(14) are all satisfied by solution P. Thus P is a feasible solution to problem(*RLX*), which concludes the proof. ■

Lemma 4. *In terms of problem(RLX), as long as the total sojourn durations $\sum_{l\in N} U(x_l)$ and $\sum_{l\in N} U(\nu_l)$ at each sensor's location remains the same, the network lifetime will remain unchanged regardless of the charger's traveling path.*

Proof: Since the energy constraint Eq. (8) is relaxed to Eq. (14) in problem(*RLX*), the above lemma can be easily proved by analyzing sensors' energy profiles at each location, which only relates to the duration spent at sojourn/virtual point. We omit the proof here to conserve space. ■

Lemma 5. *Suppose P^* is an optimal solution of problem (RLX), which consists of ε^*_{il}, $U^*(x_l)$, μ^*_{il}, $U^*(\nu_l)$, η^*_i, H^*_i, τ^*_i, T^*_0 and the maximum network lifetime $T^* = \sum_{l\in N}[U^*(x_l) + U^*(\nu_l)]$. We can always construct a solution of problem(LP-T) with the network lifetime $T^{'} \geq T^*$.*

Proof: Based on lemma 4, we can regulate the charger's traveling path to a single TSP path ($L = N$), and then problem(*RLX*) can be solved by CPLEX. Denote the resulted solution as P^*.

Next, we construct a solution $\overline{P}$ as follows: we keep the charger traveling path, sojourn and traveling durations unchanged while data routing is altered to the minimum energy routing. Specifically, $\overline{P}$ consists of ε_{il}, $U^*(x_l)$, μ_{il}, $U^*(\nu_l)$, η_i, H_i, τ_i, T_0 and $\overline{T}$ (note that $\overline{T} = T^*$). Suppose the total energy consumption of solution P^* and $\overline{P}$ during the operational interval are ω^* and ω, respectively. To prove lemma 5, we need to prove: (i) $\omega^* \geq \omega$; (ii) $T^*_0 \geq T_0$; (iii) For P^*, Eq. (9) reaches equality.

(i) Based on the definition of ω^* and ω, we have:

$$\omega^* = \sum_{i\in N}\sum_{l\in N} e^*_{il} \quad \text{and} \quad \omega = \sum_{i\in N}\sum_{l\in N} e_{il}$$

where

$$e^*_{il} = (\varepsilon^*_{il} + \mu^*_{il}\lambda_l)U^*(x_l) + [U^*(\nu_l) - \lambda_l U^*(x_l)]\eta^*_i$$

and

$$e_{il} = (\varepsilon_{il} + \mu_{il}\lambda_l)U^*(x_l) + [U^*(\nu_l) - \lambda_l U^*(x_l)]\eta_i$$

Solution $\overline{P}$ adopts the minimum energy routing during the whole network lifetime, therefore, for any $l \in L$, we have $\sum_{i\in N}\varepsilon_{il} \leq \sum_{i\in N}\varepsilon^*_{il}$, $\sum_{i\in N}\mu_{il} \leq \sum_{i\in N}\mu^*_{il}$ and $\sum_{i\in N}\eta_i \leq \sum_{i\in N}\eta^*_i$. Thus, we have

$$\begin{aligned}\omega^* - \omega = \sum_{l\in N}\{&(\sum_{i\in N}\varepsilon^*_{il} - \sum_{i\in N}\varepsilon_{il})U^*(x_l)\\ &+ (\sum_{i\in N}\mu^*_{il} - \sum_{i\in N}\mu_{il})\lambda_l U^*(x_l)\\ &+ (\sum_{i\in N}\eta^*_i - \sum_{i\in N}\eta_i)[U^*(\nu_l) - \lambda_l U^*(x_l)]\} \geq 0\end{aligned}$$

(ii) Based on the fact that total energy assumption equals to total energy allocation, we have:

$$\omega^* + Ne_0T^*_0 = Nh_0 + \varpi_0\sum_{i\in N}\tau^*_i + \varpi\sum_{i\in N}U^*(x_i) \quad (20)$$

and

$$\omega + Ne_0T_0 = Nh_0 + \varpi_0\sum_{i\in N}\tau_i + \varpi\sum_{i\in N}U^*(x_i) \quad (21)$$

Let Eq. (20) minus Eq. (21), we can obtain

$$(\varpi_0 - Ne_0)(\sum_{i\in N}\tau^*_i - \sum_{i\in N}\tau_i) = \omega^* - \omega \geq 0$$

The charging rate during initial time ϖ_0 is larger than the total energy consumption rate, namely, $\varpi_0 - Ne_0 > 0$. Otherwise, sensor batteries may deplete before the beginning of operational interval T_0. Thus we obtain $\sum_{i\in N}\tau^*_i \geq \sum_{i\in N}\tau_i$. Based on $T_0 = t_{TL} + \sum_{i\in N}\tau_i$, we can derive $T^*_0 \geq T_0$.

(iii) It can be explained intuitively. Suppose the equality is not reached, which means that a part of energy is unallocated. Then, we can always find a method to reallocate the unallocated energy and obtain a longer T, which contradicts the fact that T^* is the maximum network lifetime. Thus we have:

$$Nh_0 + \varpi_0\sum_{i\in N}\tau^*_i + \varpi\sum_{l\in N}U^*(x_l) = E$$

The above equation is based on the fact that we are in full charge of energy allocation of the sensor network. To prove lemma 5, we first need to prove that $\overline{P}$ is a feasible solution of problem(*LP-T*). Since H_i is a intermediate parameter that can be removed by reformulation and $U^*(\nu_l) \geq \lambda_l U^*(x_l)$ holds, we only need to prove that Eq. (9) is satisfied by $\overline{P}$. Based on (i) and (ii), we can derive:

$$\begin{aligned}&Nh_0 + \varpi_0\sum_{i\in N}\tau_i + \varpi\sum_{l\in N}U^*(x_l) = \omega + Ne_0T_0\\ &\leq \omega^* + Ne_0T^*_0 = Nh_0 + \varpi_0\sum_{i\in N}\tau^*_i + \varpi\sum_{l\in N}U^*(x_l) = E\end{aligned}$$

Thus $\overline{P}$ is feasible to problem(*LP-T*). The above equation also shows that a part of energy is unallocated in solution $\overline{P}$. Based on (iii), we can always construct a solution of problem(*LP-T*) with longer network lifetime $T^{'} \geq \overline{T} = T^*$, which concludes the proof. ■

Finally, we prove theorem 3.

Proof: Suppose P^* is an optimal solution of problem (*RLX*) with the maximum network lifetime T^*. Based on lemma 5, we can always construct a solution of problem(*LP-T*), say $\overline{P}$, with a network lifetime $\overline{T} \geq T^*$. Meantime, based

on lemma 3, solution $\overline{P}$ is also feasible to problem(*RLX*). And the maximum network lifetime of problem(*RLX*) is T^*. Hence, solution $\overline{P}$ is also the optimal solution of problem(*RLX*) with the network lifetime $\overline{T} = T^*$, which concludes the proof. ■

APPENDIX E
PROOF OF THEOREM 4

Proof: As to $W = 1$, problem(*LP-W*) equals to problem(*LP-T*). Here, we emphasize on the $W > 1$ situation. Let $U^w(x_l) = WU(x_l)$ and $U^w(\nu_l) = WU(\nu_l)$, then the objective function of problem(*LP-W*) becomes

$$T = \sum_{l \in N} [U^w(x_l) + U^w(\nu_l)] \tag{22}$$

And constraint Eq. (17) is converted to:

$$\sum_{l \in N} e_{il}^w - \varpi U^w(x_i) = H_i \tag{23}$$

where

$$e_{il}^w = \varepsilon_{il} U^w(x_l) + \mu_{il} \lambda_l U^w(x_l) + (U^w(\nu_l) - \lambda_l U^w(x_l))\eta_i$$

Similarly, constraint Eq. (18) is converted to:

$$N h_0 + \varpi_0 \sum_{i \in N} \tau_i + \varpi \sum_{l \in N} U^w(x_l) \leq E \tag{24}$$

Then, based on the new objective function Eq. (22) and constraints Eq. (23) (24), problem(*LP-W*) can be equivalently transformed to problem(*LP-T*), which concludes the proof. ■